

# The electric dipole moment and hyperfine interactions of KOH

J. Cederberg and D. Olson

*Department of Physics, St. Olaf College, Northfield, Minnesota 55057*

D. Rioux

*Department of Physics, University of Wisconsin-Oshkosh, Oshkosh, Wisconsin 54901*

T. Dillemoth

*2408 Springdale Rd, Apt. 16, Waukesha, Wisconsin 53186*

B. Borovsky

*Department of Physics, University of Minnesota, Minneapolis, Minnesota 55455*

J. Larson

*Department of Mechanical Engineering, University of Minnesota, Minneapolis, Minnesota 55455*

S. Cheah

*Knox College, Galesburg, Illinois 61401*

M. Carlson and M. Stohler

*Department of Physics, St. Olaf College, Northfield, Minnesota 55057*

(Received 22 April 1996; accepted 20 May 1996)

A molecular beam spectrometer has been used to observe the hyperfine spectrum and determine the electric dipole moment of the KOH molecule. This EDM had never been measured previously, although theoretical calculations had been made. A refined line shape fitting procedure has helped make possible this determination from the molecular beam hyperfine spectrum. The value of the EDM, which we found for the ground vibrational state, is  $7.415 \pm 0.002$  debye. The hyperfine constants, including the potassium nuclear quadrupole, both spin-rotation interactions, and the tensor and scalar spin-spin interactions have been determined for several vibrational states.

© 1996 American Institute of Physics. [S0021-9606(96)00433-3]

## I. INTRODUCTION

The molecule KOH has been the subject of numerous spectroscopic studies over the past 30 years, which have steadily expanded the understanding of its structure. Its linearity has been established, and measurements have been made of the rotational constant and its dependence on vibrational state.<sup>1-5</sup> Microwave measurements with sufficient precision to give a value for the potassium nuclear quadrupole interaction have been reported.<sup>6-9</sup> Theoretical calculations, but no previous experimental measurements have been made for the electric dipole moment.<sup>10,11</sup>

We have used a high-resolution molecular beam electric resonance spectrometer to examine the hyperfine spectrum and in the process have also completed the first measurement of its intrinsic electric dipole moment. We have been able to observe pure hyperfine transitions in rotational states  $J=1-4$ , vibrational states  $(v_1, v_2^l, v_3) = (0, 0^0, 0), (1, 0^0, 0), (2, 0^0, 0), (3, 0^0, 0),$  and  $(0, 2^0, 0)$ . Preliminary reports of our work have been given at conferences.<sup>12,13</sup>

## II. THE SPECTRUM

To first approximation the KOH molecule is very similar to KF.<sup>14</sup> The OH radical has the same number of electrons as fluorine, nearly the same mass, and the same nuclear spin. The OH is tightly enough bound that the OH stretching vibration modes are not significantly excited at the temperature of our source. The field gradient at the potassium nucleus is

also about the same in both molecules. We therefore expected to see a hyperfine spectrum which was much like that for KF.

The transitions which we observed are pure hyperfine transitions, involving changes in the relative orientations of the nuclear and rotational angular momenta. They do not change the vibrational ( $v$ ) or rotational ( $J$ ) quantum numbers, so that the thermal populations established at the oven temperature are maintained. Since the rotational state does not change, these transitions violate the angular momentum selection rule for first order electric dipole transitions. They nevertheless occur by a process which can be thought of as involving two photons, usually with one at the frequency of the oscillating electric field, and one at the zero frequency of the applied dc field.

The observed spectrum has the structure shown in Figs. 1-3. There are groups of lines in the frequency ranges 1800-1900 kHz (which includes all rotational states), a  $J=1$  group in the range 3300-3400 kHz, a  $J=2$  group between 3050 and 3250 kHz, a  $J=3$  group between 2700 and 2800 kHz, etc. Within each of these groups there is a strongest set, which we take to be the ground vibrational state, repeated in a sequence moving toward lower frequency that decreases exponentially in amplitude. We assume that this sequence is formed by the excited states of the K-O stretch, just like the sequence of lines found in KF. Exciting the higher states of this vibration increases the average bond length, and reduces the field gradient. This is confirmed by the match of the

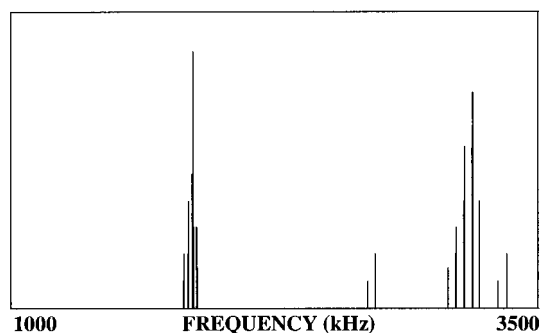


FIG. 1. Initially observed spectrum.

amplitude ratio for successive sets of the sequence with the Boltzmann factor for the vibrational states at the temperature of our source. Each set contains three lines (more for the 1800–1900 kHz group), just as they did for KF, though with a different order and smaller separation.

There was another feature, however, which was not present in the KF spectrum. There is another set of lines within each group, displaced toward higher frequencies, but smaller in amplitude than the set for the ground vibrational state, as visible at the far right in Fig. 3. These we believe to be due to the  $(0,2^0,0)$  excited bending mode of the molecule. The  $l \neq 0$  bending modes apparently cannot be observed in our pure hyperfine spectrum because they are saturated by the greatly over-driven first order transitions between these  $l$  doublet pairs of states. The  $l$  doublet transitions also were likely responsible for a very large background signal which was present in our hyperfine data. Again, the ratio of intensity to that of the ground vibrational state confirmed that this is the correct interpretation. The higher frequency of the  $(0,2^0,0)$  set means that the electric field gradient at the K nucleus is greater for this excited bending mode than it is in the ground vibrational state. This contrasts with the fact that the rotational constant decreases with excitation of both the stretching mode and the bending mode.

In addition to the pure hyperfine transitions, we were able to observe two lines which occur between the  $l$  doublet states, at approximately 31 378.3 and 31 315.6 kHz, but were unable to identify the states involved. These are allowed, single-photon transitions so that the required amplitude of the oscillating electric field is much smaller than for the pure hyperfine transitions. The extreme broadening of these transitions at the field levels used for the pure hyperfine transitions probably accounts for the very high background levels that we consistently observed in the 1000–3500 kHz range.

The order and separation of the three lines within each set, which is determined primarily by the hydrogen spin-rotation interaction, indicates that this interaction has the opposite sign and is smaller by about an order of magnitude than the corresponding interaction of fluorine in KF.

These qualitative conclusions follow from the overall appearance of the spectrum. The quantitative analysis, which gives the numerical values of the hyperfine interactions and the electric dipole moment, is described in the next section.

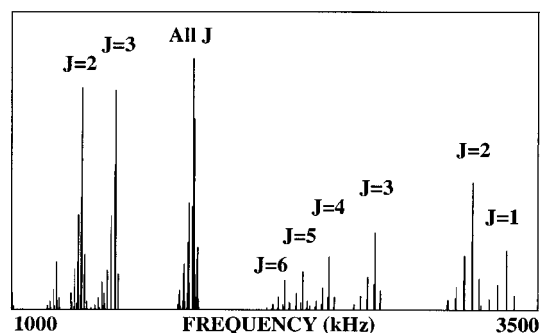


FIG. 2. Spectrum predicted from final fitted frequencies.

### III. ANALYSIS

Most of our measurements were made using a pair of electrostatic quadrupole lenses which were 29 cm long. These worked well for the rotational states  $J=2-3$ , but not for  $J=1$  (for which the inception of the fourth order Stark effect causes the lens to become defocusing for all values of  $m_J$ ) or for  $J \geq 4$  (for which arcing prevents sufficient potential from being applied). Near the end of the project a longer (43 cm) set of lenses was made and installed to permit the examination of transitions in  $J=1$  and 4. Our initial fitting and analysis thus concentrated on the  $J=2-3$  states.

The Hamiltonian used was of the form

$$H = H_{\text{elect}} + H_{\text{vib}} + H_{\text{rot}} + H_{\text{hyperfine}} + H_{\text{stark}}, \quad (1)$$

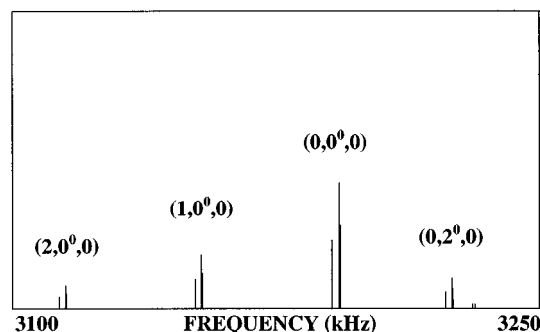
where

$$H_{\text{hyperfine}}/h = \mathbf{V}_K \cdot \mathbf{Q}_K + c_K \mathbf{I}_K \cdot \mathbf{J} + c_H \mathbf{I}_H \cdot \mathbf{J} + c_3 \mathbf{I}_K \cdot \mathbf{D} \cdot \mathbf{I}_H + c_4 \mathbf{I}_K \cdot \mathbf{I}_H \quad (2)$$

and

$$H_{\text{Stark}} = -\boldsymbol{\mu} \cdot \mathbf{E}. \quad (3)$$

Since the hyperfine Hamiltonian is dominated by the first term, representing the electric quadrupole interaction of the potassium nucleus, the most appropriate zero-field coupling scheme is that defined by the relations

FIG. 3. Detail from Fig. 2 showing the predicted spectrum for the  $J=2$  group of lines. There are three lines within each vibrational set.

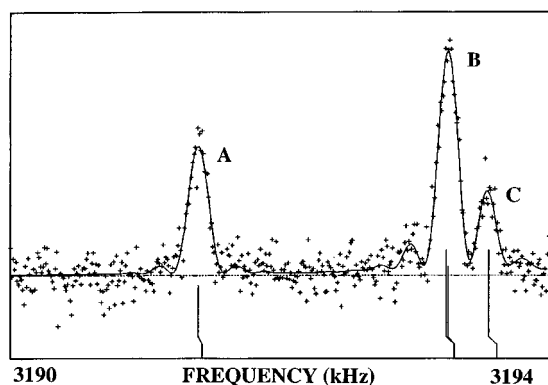


FIG. 4. Experimental data and fit for the  $(v_1, v_2, v_3) = (0, 0^0, 0)$ ,  $J=2$  set of three lines. Line identifications, in the form  $F_1, F \rightarrow F'_1, F'$ , are A:  $1/2, 1 \rightarrow 5/2, 2$ ; B:  $1/2, 1 \rightarrow 5/2, 3$ , and C:  $1/2, 0 \rightarrow 5/2, 2$ .

$$\mathbf{F}_1 = \mathbf{J} + \mathbf{I}_K, \quad \mathbf{F} = \mathbf{F}_1 + \mathbf{I}_F. \quad (4)$$

Because of the small value of the hydrogen spin-rotation interaction, some of the hyperfine lines were not completely resolved, and furthermore, the Stark effect caused a mixing of the hyperfine states even at the smallest fields needed to produce transitions. To fully take this into account, we used a line shape analysis procedure described previously.<sup>15</sup> The zero-field hyperfine Hamiltonian matrix was found for each vibrational-rotational state using initial guess values of the hyperfine constants and dipole moment. Corrections were applied to the level of third order perturbation to include the effect of the coupling between rotational states  $J$  and  $J' = J \pm 2$  by the nuclear quadrupole interaction. The eigenvalues and eigenvectors of these matrices were found, along with the effective Stark matrix, as expressed in the representation which diagonalizes the zero-field Hamiltonian. The effective Stark Hamiltonian was then evaluated for the fields used in the transition, and the Hamiltonian for hyperfine plus Stark interactions rediagonalized. The final eigenvalues were the Stark shifted energies, and the eigenvectors were used to find the transition probabilities between the Stark-mixed states.

In order to find an accurate velocity distribution of the molecules as focused by the lenses, a computer program was used to track the trajectories in the transverse phase space as they move through the different parts of the apparatus.<sup>16</sup> In this way, the fraction that were expected to be focused on the detector could be calculated for a range of longitudinal speeds. This was combined with the Boltzmann distribution of the speeds leaving the oven to give the complete velocity distribution. The observed line shape corresponds to the Rabi function summed over the velocity distribution.

With a known line shape, each observed line, including all its Stark components, was fitted using a simplex method with only three variable parameters: the zero-field frequency, the amplitude, and the background. If multiple transitions occurred in the range of an experimental run, they could be fitted with separate zero-field frequencies, but a common background. The amplitudes could be varied independently,

TABLE I. Molecular constants obtained from fit (in kHz).

Constant	Coefficient of			
	$(v_1 + 1/2)$	$(v_1 + 1/2)^2$	$J(J+1)$	$(v_2 + 1)$
<i>K</i> quadrupole				
-7462.018	94.188	-0.986	0.0285	-37.451
$\pm 0.032^a$	$\pm 0.062$	$\pm 0.022$	$\pm 0.0033$	$\pm 0.045$
<i>K</i> spin-rotation				
0.2124				
$\pm 0.0025$				
<i>H</i> spin-rotation				
-0.9920	0.0293			0.0564
$\pm 0.0049$	$\pm 0.0035$			$\pm 0.012$
Spin-spin tensor				
0.1748				
$\pm 0.0052$				
Spin-spin scalar				
0.0115				
$\pm 0.0034$				
Dipole moment (debye):				
7.263	0.069	-0.004		0.1185
$\pm 0.012$	$\pm 0.025$	$\pm 0.010$		$\pm 0.0059$
Dipole moments determined for individual vibrational states				
State	Dipole moment		Rotational constant (MHz)	
$(0, 0^0, 0)$	$7.415 \pm 0.002^a$		$8208.6655 \pm 0.0016^b$	
$(1, 0^0, 0)$	$7.476 \pm 0.007$		$8142.656 \pm 0.008^c$	
$(2, 0^0, 0)$	$7.529 \pm 0.014$		$8076.698 \pm 0.018^c$	
$(0, 2^0, 0)$	$7.652 \pm 0.004$		$8135.1632 \pm 0.0028^b$	

<sup>a</sup>Our quoted uncertainties are one standard deviation estimates. Cited uncertainties for rotational constants are three standard deviations.

<sup>b</sup>Y. Kawashima, R. D. Suenram, and E. Hirota, *J. Mol. Spectrosc.* **175**, 99 (1996).

<sup>c</sup>E. F. Pearson, B. P. Winnewisser, and M. B. Trueblood, *Z. Naturforsch. Teil A* **31**, 1259 (1976).

but in practice were found to be rather similar, reflecting the thermal populations of the different states. Other parameters which we had previously treated as variables determined by the fit, such as the time of passage through the transition region, or the probability of transition, were reduced to predictions by the above procedure.

In order for this procedure to accurately correct for the Stark shifts in the line positions, the electric dipole moment and the rotational constant must be known. Rotational constant values in different vibrational states had been reported, but no values of the dipole moment were available. We therefore made a series of observations at different fields, using the line  $J=2$ ,  $(F_1, F) = (1/2, 1) \rightarrow (5/2, 2)$ , because it is isolated, has a single Stark component, and shows a sizable Stark shift. This is the lowest frequency line of the set of three shown for each vibrational state in Fig. 3. We fit each measurement starting with a range of initial guesses of the dipole moment. The correct value of the dipole moment would give no shift in the zero-field frequency as the field was increased. With this dipole moment value determined, the other lines of the spectrum could also be fitted giving consistent zero-field frequencies independent of the actual

TABLE II. Comparison of observed and fitted frequencies.

$(v_1, v_2, v_3)$	$J$	$F_1, F \rightarrow F_1, F$	Measured freq. (kHz)	Uncert. <sup>a</sup>	Predicted frequency	Resid.	Ratio resid/uncert
(0,0 <sup>0</sup> ,0)	1	1/2,1→5/2,3	1490.312	0.020	1490.2911	0.0210	1.05 <sup>b</sup>
(0,0 <sup>0</sup> ,0)	1	1/2,1→5/2,2	1489.345	0.020	1489.3325	0.0125	0.62 <sup>b</sup>
(0,0 <sup>0</sup> ,0)	1	1/2,1→3/2,2	3353.830	0.010	3353.8354	-0.0054	-0.54 <sup>b</sup>
(0,0 <sup>0</sup> ,0)	1	1/2,1→3/2,1	3353.043	0.010	3353.0442	-0.0012	-0.12 <sup>b</sup>
(1,0 <sup>0</sup> ,0)	1	1/2,1→3/2,1	3311.600	0.045	3311.5518	0.0482	1.07
(0,0 <sup>0</sup> ,0)	1	1/2,0→5/2,2	1488.601	0.030	1488.5826	0.0183	0.61 <sup>b</sup>
(0,0 <sup>0</sup> ,0)	1	1/2,0→3/2,2	3353.085	0.015	3353.0854	-0.0004	-0.03 <sup>b</sup>
(0,0 <sup>0</sup> ,0)	2	7/2,4→5/2,3	1863.818	0.030	1863.7902	0.0275	0.92 <sup>b</sup>
(0,0 <sup>0</sup> ,0)	2	7/2,3→5/2,3	1865.700	0.030	1865.7042	-0.0042	-0.14 <sup>b</sup>
(0,0 <sup>0</sup> ,0)	2	7/2,3→5/2,2	1863.924	0.100	1863.8224	0.1010	1.01 <sup>b</sup>
(0,0 <sup>0</sup> ,0)	2	1/2,1→5/2,3	3193.310	0.015	3193.3070	0.0028	0.18 <sup>b</sup>
(1,0 <sup>0</sup> ,0)	2	1/2,1→5/2,3	3153.786	0.016	3153.7774	0.0086	0.54 <sup>b</sup>
(2,0 <sup>0</sup> ,0)	2	1/2,1→5/2,3	3115.088	0.020	3115.0931	-0.0051	-0.25 <sup>b</sup>
(3,0 <sup>0</sup> ,0)	2	1/2,1→5/2,3	3077.400	0.050	3077.2540	0.1460	2.92
(0,0 <sup>0</sup> ,0)	2	1/2,1→5/2,2	3191.430	0.010	3191.4252	0.0048	0.48 <sup>b</sup>
(1,0 <sup>0</sup> ,0)	2	1/2,1→5/2,2	3151.934	0.013	3151.9509	-0.0172	-1.32 <sup>b</sup>
(2,0 <sup>0</sup> ,0)	2	1/2,1→5/2,2	3113.321	0.010	3113.3218	-0.0008	-0.08 <sup>b</sup>
(3,0 <sup>0</sup> ,0)	2	1/2,1→5/2,2	3075.600	0.100	3075.5380	0.0620	0.62
(0,0 <sup>0</sup> ,0)	2	1/2,1→3/2,2	1862.812	0.020	1862.8287	-0.0167	-0.83 <sup>b</sup>
(1,0 <sup>0</sup> ,0)	2	1/2,1→3/2,2	1839.755	0.010	1839.7731	-0.0181	-1.81
(0,0 <sup>0</sup> ,0)	2	1/2,1→3/2,1	1861.078	0.015	1861.0812	-0.0032	-0.21 <sup>b</sup>
(1,0 <sup>0</sup> ,0)	2	1/2,1→3/2,1	1838.046	0.010	1838.0724	-0.0264	-2.64
(0,0 <sup>0</sup> ,0)	2	1/2,0→5/2,2	3193.627	0.015	3193.6278	-0.0005	-0.03 <sup>b</sup>
(1,0 <sup>0</sup> ,0)	2	1/2,0→5/2,2	3154.105	0.014	3154.0948	0.0102	0.73 <sup>b</sup>
(2,0 <sup>0</sup> ,0)	2	1/2,0→5/2,2	3115.410	0.020	3115.3620	0.0029	0.14
(3,0 <sup>0</sup> ,0)	2	1/2,0→5/2,2	3077.750	0.100	3077.5647	0.1853	1.85
(0,0 <sup>0</sup> ,0)	2	1/2,0→3/2,2	1865.028	0.020	1865.0312	-0.0036	-0.18 <sup>b</sup>
(0,0 <sup>0</sup> ,0)	3	9/2,5→7/2,4	1864.025	0.100	1863.9947	0.0303	0.30
(0,0 <sup>0</sup> ,0)	3	9/2,4→7/2,4	1866.878	0.250	1866.8512	0.0264	0.11 <sup>b</sup>
(0,0 <sup>0</sup> ,0)	3	9/2,4→7/2,3	1864.239	0.100	1863.9673	0.2717	2.72
(0,0 <sup>0</sup> ,0)	3	3/2,2→7/2,4	2731.283	0.010	2731.2831	-0.0001	-0.01 <sup>b</sup>
(1,0 <sup>0</sup> ,0)	3	3/2,2→7/2,4	2697.450	0.100	2697.4664	-0.0164	-0.16
(0,0 <sup>0</sup> ,0)	3	3/2,2→7/2,3	2728.395	0.010	2728.3993	-0.0043	-0.43 <sup>b</sup>
(0,0 <sup>0</sup> ,0)	3	3/2,2→5/2,3	1862.500	0.010	1862.4974	0.0026	0.26 <sup>b</sup>
(1,0 <sup>0</sup> ,0)	3	3/2,2→5/2,3	1839.451	0.005	1839.4436	0.0077	1.68
(0,0 <sup>0</sup> ,0)	3	3/2,2→5/2,2	1859.631	0.050	1859.5701	0.0609	1.22 <sup>b</sup>
(1,0 <sup>0</sup> ,0)	3	3/2,2→5/2,2	1836.619	0.025	1836.6016	0.0174	0.70 <sup>b</sup>
(2,0 <sup>0</sup> ,0)	3	3/2,2→5/2,2	1814.141	0.025	1814.1262	0.0148	0.59 <sup>b</sup>
(0,0 <sup>0</sup> ,0)	3	3/2,1→7/2,3	2731.694	0.010	2731.6954	-0.0014	-0.14 <sup>b</sup>
(0,0 <sup>0</sup> ,0)	3	3/2,1→5/2,3	1865.784	0.010	1865.7935	-0.0095	-0.95
(0,0 <sup>0</sup> ,0)	3	3/2,1→5/2,2	1862.880	0.020	1862.8661	0.0139	0.69 <sup>b</sup>
(0,0 <sup>0</sup> ,0)	4	5/2,3→9/2,5	2514.560	0.040	2514.5549	0.0056	0.14 <sup>b</sup>
(0,0 <sup>0</sup> ,0)	4	5/2,2→9/2,4	2514.940	0.040	2514.9844	-0.0446	-1.12 <sup>b</sup>
(0,2 <sup>0</sup> ,0)	2	1/2,1→5/2,3	3225.367	0.020	3225.3662	0.0008	0.04 <sup>b</sup>
(0,2 <sup>0</sup> ,0)	2	1/2,1→5/2,2	3223.762	0.005	3223.7620	-0.0000	-0.00 <sup>b</sup>
(0,2 <sup>0</sup> ,0)	2	1/2,0→5/2,2	3225.670	0.010	3225.6702	-0.0002	-0.02 <sup>b</sup>

<sup>a</sup>Uncertainties are 1 standard deviation estimates.<sup>b</sup>Measurements included in fit. Other lines were observed initially but not later confirmed.

field used. In a similar manner, the dipole moments were determined for the other observed vibrational states. Figure 4 shows an example of the fit of the set of three lines for the  $J=2$ ,  $(v_1, v_2, v_3) = (0, 0^0, 0)$  state.

The accuracy of our dipole moment value was limited by the accuracy and uniformity of the spacing between the milled and lapped aluminum plates that form our C field, and by our knowledge of the potential difference between the plates. The latter was set by a 12 bit D–A converter dividing a 10 V reference, which then controlled a 100 V power sup-

ply. In order to test these, we observed similar transitions in the KF molecule, for which the dipole moment is known. In order to fit the Stark shifts observed in KF, we had to apply a small correction of about 0.25%. Our quoted dipole moment values take this correction into account.

With the Stark shifts more accurately accounted for, our zero-field frequencies could be used in a fit to improve the values of the hyperfine constants. This iterative process was repeated several times as additional lines were observed and identified. The final list of measured zero-field frequencies is

shown in Table II, along with the predictions given by the molecular constants listed in Table I.

#### IV. CONCLUSION

We have determined the values of the standard hyperfine constants for potassium hydroxide, namely the potassium nuclear quadrupole constant, the two spin-rotation constants, and the tensor and scalar spin-spin constants. A magnetic octupole interaction for the potassium nucleus would be possible, but we have not seen, and would not expect, any significantly nonzero effect. Our value of the quadrupole constant is consistent with, but much more precise than, previous measurements, and includes the dependence on both stretching and bending modes of vibration. The fact that it increases with bending mode excitation is especially interesting. Our values of the other constants are new. The negative sign of the hydrogen spin-rotation constant came as a surprise to us, since it is opposite to that of fluorine in KF.

We have also measured the electric dipole moment for the first time. We can represent the dipole moment for the different values of  $v_1$  and  $v_2$  by the expansion

$$\mu_{v_1 v_2 v_3} = \mu_{ee0} + \mu_{10}(v_1 + \frac{1}{2}) + \mu_{20}(v_1 + \frac{1}{2})^2 + \mu_{01}(v_2 + 1), \quad (5)$$

but without having access to excited states of the O-H stretching mode we cannot correct for its zero-point motion to determine a true equilibrium dipole moment. Our value of  $\mu_{ee0}$  is reasonably close to the value of 7.2 debye calculated by Mestdagh *et al.*<sup>11</sup> for the equilibrium dipole moment, but much farther from the earlier calculation of 8.46 debye by England.<sup>10</sup>

#### ACKNOWLEDGMENTS

The authors wish to thank the National Science Foundation, the Research Corporation, and the Pew Foundation for support related to this work.

- <sup>1</sup>R. L. Kuczkowski, D. R. Lide, Jr, and L. C. Krisher, *J. Chem. Phys.* **44**, 3131 (1966).
- <sup>2</sup>E. F. Pearson and M. B. Trueblood, *J. Chem. Phys.* **58**, 826 (1973).
- <sup>3</sup>P. Kuijpers, T. Törring, and A. Dymanus, *Z. Naturforsch. Teil A* **30**, 1256 (1975).
- <sup>4</sup>E. F. Pearson, B. P. Winnewisser, and M. B. Trueblood, *Z. Naturforsch. Teil A* **31**, 1259 (1976).
- <sup>5</sup>P. Kuijpers, T. Törring, and A. Dymanus, *Z. Naturforsch. Teil A* **32**, 930 (1977).
- <sup>6</sup>T. T. Raw, T. Yamamura, and C. W. Gillies, *Rev. Sci. Instrum.* **58**, 979 (1987).
- <sup>7</sup>T. T. Raw, T. Yamamura, and C. W. Gillies, *J. Chem. Phys.* **87**, 3706 (1987).
- <sup>8</sup>Y. Kawashima, R. D. Suenram, and E. Hirota, Paper MG11, Symposium on Molecular Spectroscopy, The Ohio State University (1994).
- <sup>9</sup>Y. Kawashima, R. D. Suenram, and E. Hirota, *J. Mol. Spectrosc.* **175**, 99 (1996).
- <sup>10</sup>W. B. England, *J. Chem. Phys.* **68**, 4896 (1978).
- <sup>11</sup>J. M. Mestdagh and J. P. Visticot, *Chem. Phys.* **155**, 79 (1991).
- <sup>12</sup>J. Cederberg, D. Rioux, D. Nitz, and D. Olson, Paper TA8, Symposium on Molecular Spectroscopy, The Ohio State University (1988).
- <sup>13</sup>J. Cederberg, D. Olson, D. Laine, S. Cheah, P. Zimmer, D. Rioux, B. Borovsky, and M. Carlson, Paper RK06, Symposium on Molecular Spectroscopy, The Ohio State University (1995).
- <sup>14</sup>G. Paquette, A. Kotz, J. Cederberg, D. Nitz, A. Kolan, D. Olson, K. Gunderson, S. Lindaas, and S. Wick, *J. Mol. Structure* **190**, 143 (1988).
- <sup>15</sup>D. Olson, J. Cederberg, P. Soulen, H. Ton, K. Urberg, and B. Mock, *J. Mol. Spectrosc.* **166**, 158 (1994).
- <sup>16</sup>J. Cederberg, D. Olson, and J. Larson, Paper RK07, Symposium on Molecular Spectroscopy, The Ohio State University (1995).

The Journal of Chemical Physics is copyrighted by the American Institute of Physics (AIP). Redistribution of journal material is subject to the AIP online journal license and/or AIP copyright. For more information, see <http://ojps.aip.org/jcpo/jcpcr/jsp>  
Copyright of Journal of Chemical Physics is the property of American Institute of Physics and its content may not be copied or emailed to multiple sites or posted to a listserv without the copyright holder's express written permission. However, users may print, download, or email articles for individual use.